ISBN: 978-3-95450-238-7 ISSN: 2226-0358 doi:10.18429/JACoW-ICALEPCS2023-TUPDP020

SUMMARY REPORT ON MACHINE LEARNING-BASED APPLICATIONS AT THE SYNCHROTRON LIGHT SOURCE DELTA

D. Schirmer*, S. Khan, A. Radha Krishnan
Center for Synchrotron Radiation (DELTA), TU Dortmund University, Germany

Abstract

In recent years, several control system applications using machine learning (ML) techniques have been developed and tested to automate the control and optimization of the 1.5 GeV synchrotron radiation source DELTA. These applications cover a wide range of tasks, including electron beam position correction, working point control, chromaticity adjustment, injection process optimization, as well as CHG spectra (coherent harmonic generation) analysis. Various machine learning techniques were utilized to implement these projects. This report provides an overview of the projects, outlines the basic concepts, and identifies ideas for future developments.

INTRODUCTION

This article presents a general overview of recent advancements in the application of machine learning (ML) techniques for accelerator control and CHG (coherent harmonic generation) spectral analysis at the 1.5 GeV synchrotron light source DELTA [1–3].

The first study demonstrates the successful implementation of neural networks (NNs) for the correction of electron beam trajectories (orbits). These networks were trained using measured beam position data and corresponding corrector magnet strengths, showcasing competitive results but with fewer correction steps compared to conventional orbit correction methods.

In a parallel effort, ML-driven techniques were employed to control the working point (betatron tunes in both orbit planes). Therefore, a classical Proportional-Integral-Derivative (PID) system was replaced on a test basis by ML-trained NNs.

The paper further explores ML-based methods for adjusting storage ring chromaticity values. Gaussian Process Regressors (GPRs) and NNs were trained as surrogate models to predict optimal sextupole magnet settings using statistical and heuristic algorithms. Results showed significant improvements in chromaticity control within few iterations compared to manually performed settings.

Additionally, a novel approach was employed to optimize injection efficiency from the booster synchrotron BoDo to the storage ring. Through ML-trained predictive models in combination with heuristic optimization algorithms, injection settings were dynamically adjusted, resulting in improved electron transfer rates.

Lastly, the paper outlines the analysis of CHG-induced radiation spectra. CHG-generated ultrashort light pulses were examined through convolutional neural networks (CNNs) to predict certain seeding laser settings from spectral measurements. This approach enabled the adjustment of the seeding laser parameters in order to optimize the spectra properties.

* detlev.schirmer@tu-dortmund.de

ORBIT CORRECTION

At DELTA, the orbit is measured at 54 locations around the storage ring roughly every second using multiplexed beam position monitor (BPM) pick-up signals. Unwanted deviations of the beam position with respect to the ideal reference orbit are minimized by 56 corrector magnets, 30 for the horizontal plane (x) and 26 for the vertical plane (y). They are operated by a ‘slow’ (approx. 1 Hz) software feedback system applying numerical algorithms such as the SVD-method (singular value decomposition) [4] or the IPM-based (interior point-proximal method) software [5].

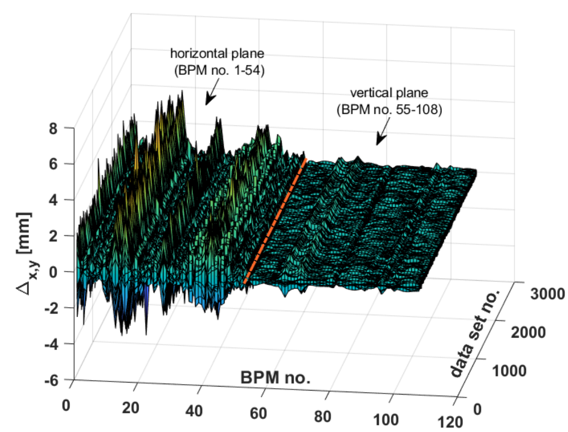

Figure 1: Orbit response at 108 BPM signals for the simulated x,y-coupled DELTA storage ring, calculated for 54 horizontal (x) and 54 vertical (y) deviations. In this example, 3000 randomly disturbed orbit vectors are shown. The data sets are used as inputs for supervised training of NNs.

As an alternative method, flat, non-deep NNs have been investigated for automatic orbit correction. ML-based studies on this topic, which initially were based on simulations (e.g., see Figs. 1 and 2), have then been successfully transferred to real accelerator operation. For this purpose, classical fully connected multi-layer feed-forward networks with more than 17.000 links were trained using supervised learning with measured beam position data and corresponding corrector magnet strengths. The trained networks subsequently served as inverse models for local and global beam position corrections. The supervised NN training was comparatively evaluated with various back-propagation learning algorithms (e.g., see Fig. 2). Finally, the performance of the ML-based beam control was benchmarked with conven-

ISBN: 978-3-95450-238-7 ISSN: 2226-0358 doi:10.18429/JACoW-ICALEPCS2023-TUPDP020

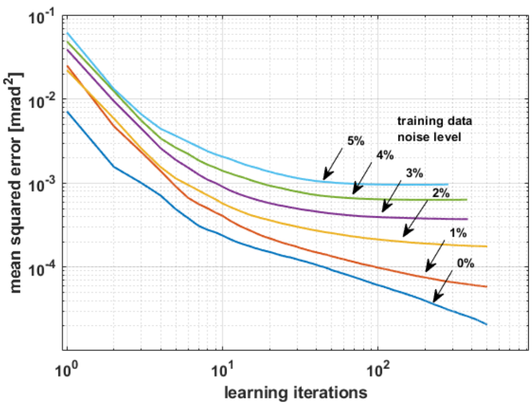

Figure 2: Network learning functions for 'unseen' validation data sets (validation curves). Each curve refers to a hidden sub-set of 300 recordings ranking the network's performance according to the mean of squared errors (mse) for 'unseen' data. In this example iterative NN learning was performed with a conjugate gradients-based back-propagation algorithm [6, 7] for various noise levels of the training data (simulation).

tional numerical-based computational methods (SVD [4], IPM [5]). Here, the ML-based approach showed competitive orbit correction quality, but generally with a lower number of iteration steps. For more details and results see [8–10].

TUNES CONTROL

The working point $Q_{x,y}$ of a storage ring, which is composed of the betatron tunes for both transverse directions, describes the number of betatron oscillations of the stored particle beam per revolution. The betatron tunes are crucial tuning parameters for stable operation and must therefore be constantly monitored and readjusted if necessary. Both values are set with the aid of beam-focusing quadrupole magnets. For this purpose, 3 horizontally and 4 vertically focusing quadrupole circuits are available, which are distributed in the arcs of the DELTA storage ring. For automatic control, a classic Proportional Integral Differential (PID) feedback system has been in operation for many years [11].

In a test scenario, this system was replaced by an ML-based control mechanism. For training data acquisition, quadrupole strengths were systematically and randomly varied (actuator data), and the corresponding tune shifts (response data) were measured. These actuator/response measurement pairs serve as labeled data for supervised training of classical, shallow, none-deep, and fully-connected feed-forward NNs. During training, the NNs 'learn' the correlation between changes in quadrupole strengths and tune shifts, and can subsequently be used as predictive models for automatic tune adjustment. An example is shown in Fig. 3. This approach was successfully applied for both the simulated virtual storage ring and in real machine operation. It was even possible to deploy surrogate models in real machine operation that had only been trained with simulated data. The results are summarized in [9, 12, 13].

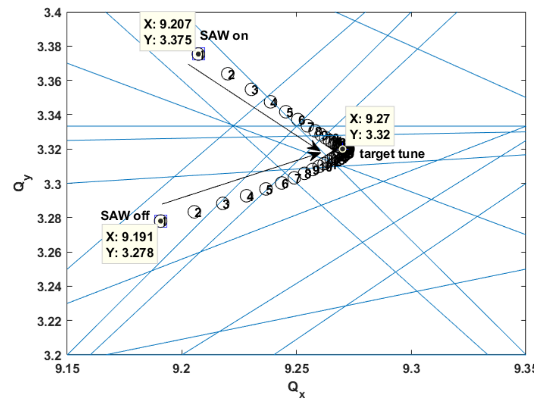

Figure 3: Two tune matching examples starting from different values with the wiggler magnet (SAW) switched on and off. The ML-based method calculates iterative shifts of the working point ($Q_{x,y}$) up to an arbitrarily chosen target tune. The blue lines indicate resonance lines in the tune diagram up to the fifth order.

CHROMATICITY ADJUSTMENT

Changes of the betatron tunes normalized to the relative momentum offset of the electron beam define the chromaticity of a storage ring. In this case, horizontally and vertically focusing sextupole magnets are utilized to variably adjust these chromaticity values within certain technical limits. For this purpose, the DELTA storage ring is equipped with a total of 13 individually controllable sextupole power supply circuits, which are software-grouped into 7 families. By default, the adjustment of the magnet circuit currents is carried out manually based on empirical knowledge.

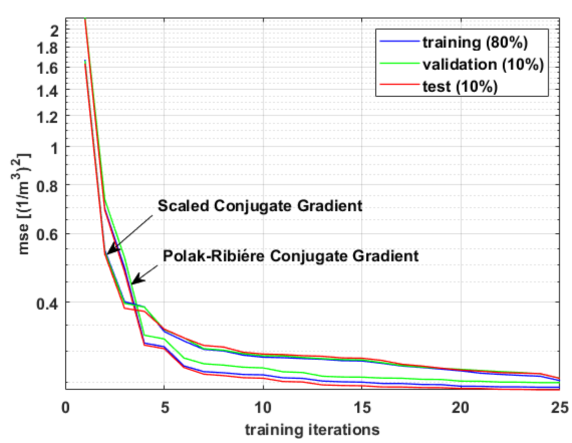

Figure 4: Comparison of network training performance functions (fitness: mean squared NN output error as a function of training iterations) with simulated data applying two different conjugate gradient back-propagation methods [6, 7]. With 80 % of the data, the network is trained (blue curve) and 20 % of the data are used for validation (10 %) and test (10 %) with 'unseen' data sets (green and red curve). The continuously falling curves indicate significant fitness improvements without over-fitting effects.

Recently, similar to the procedure for adjusting working points, an ML-based approach was utilized to automate the control in this context as well. In this case, the strengths of the sextupole magnets were varied randomly as well as systematically one by one (actuator data), and the resulting influences on the chromaticity values were measured (response data) simultaneously. NNs trained with these actuator/response data (see Fig. 4) serve as predictive models for various kinds of optimization algorithms (e.g., Bayesian optimization) to improve sextupole settings during accelerator operation. It turns out that classical ML methods applying conventional feed-forward NNs are adequate for regulating the chromaticity in both simulation and real storage ring operation. It was also shown that splitting the software-grouped sextupole powering circuits increases flexibility in achieving desired chromaticity. For more information see [14, 15].

INJECTION OPTIMIZATION

At the DELTA storage ring facility, all magnets as well as the radiofrequency power of the Booster Synchrotron (BoDo) cavity are software-controlled to cyclically ramp up and down. Each of these energy ramp cycles takes about 7 seconds, whereby the electron energy is increased from 90 MeV to 1.5 GeV. Depending on the injection efficiency and the stored beam current in BoDo, typically 150 to 200 ramp cycles are required to reach the maximum beam current of 130 mA in the storage ring. To minimize injection times, optimizing the injection efficiency from BoDo to the storage ring is crucial.

During injection, a variety of parameters must be manually adjusted, such as the strength of transfer channel magnets and trigger timings for pulsed injection and extraction

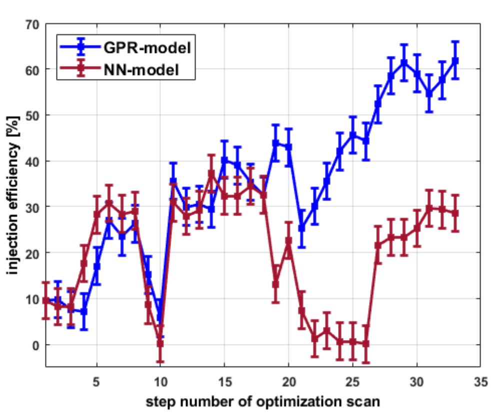

Figure 5: Examples for injection efficiency optimization scans using Bayesian optimization and applying a Gaussian Process Regressor (GPR) as a surrogate injection model (blue) in comparison to an NN-trained model (red). The best parameter set of each scan is saved and can subsequently be applied to the injection elements. Both runs started with a misadjusted injection setup with an efficiency of approx. 10 % where the GPR-based method was able to increase the value to approx. 62 %.

elements. Innovative ML concepts were tested to automate this process and improve electron transfer rates.

In two separate studies [14, 16], between 13 and 18 injection parameters were slightly varied to identify the corresponding impact on injection efficiency. In this case these measurements served as labeled data for supervised learning of different injection prediction models. In addition to NNs, decision trees (DTs) and Gaussian Process Regressors (GPR) were employed as prediction models. Heuristic (e.g. simulated annealing) and statistical (e.g. Bayesian optimization) optimization algorithms utilized these ML-based surrogate models to improve injection settings between each injection cycle. This process resulted in substantial improvements in injection efficiency for both the GPR- and NN-based models within a few injection cycles. As an example see Fig. 5. Decision trees were found to be ineffective in this area. The main results are summarized in [17].

ANALYSIS OF CHG SPECTRA

In order to generate synchrotron radiation pulses with a duration below 100 fs, coherent harmonics generation (CHG) [18] has been employed at DELTA since 2011 [2, 3]. As shown in Fig. 6, this technique uses an ultrashort seed laser pulse which interacts with the electron beam in an undulator (modulator) that is tuned to the laser wavelength. This results in a sinusoidal modulation of the electron energy, which is then converted into a density modulation using a magnetic chicane, forming microbunches separated by one laser wavelength. In a subsequent undulator (radiator), coherent emission is produced from the microbunches at harmonics of the seed laser wavelength. The coherently emitted light pulse has a pulse length comparable to the pulse length of the seed laser pulse (50 fs at DELTA short-pulse source) with wavelengths extending into the vacuum-ultraviolet range (VUV).

The spectral characteristics of the CHG radiation depends, among others, on the spectro-temporal properties of the seed laser pulse and the chicane strength. The energy modulation amplitude of the electrons follows the temporal envelope

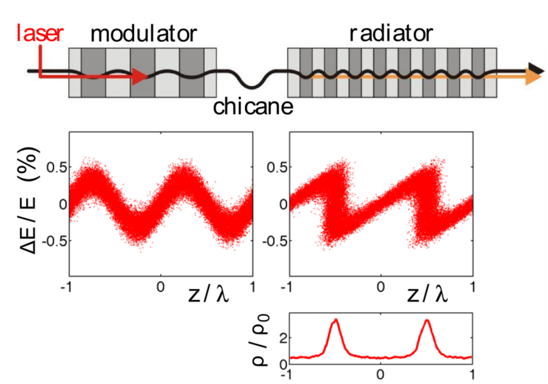

Figure 6: Magnetic setup for CHG, corresponding longitudinal phase space distributions and final longitudinal electron density.

ISBN: 978-3-95450-238-7 ISSN: 2226-0358 doi:10.18429/JACoW-ICALEPCS2023-TUPDP020

of the seed laser pulse. The spectral content of the CHG pulses also depends on the wavelength distribution along the seed laser pulse. A laser pulse with central frequency ω_0 is expressed in the frequency domain in terms of spectral amplitude $\tilde{E}(\omega)$ and spectral phase $\varphi(\omega)$ by

$$\tilde{E}(\omega) = |\tilde{E}_0(\omega)|e^{-i\varphi(\omega)}, \tag{1}$$

where $\varphi(\omega)$ can be expanded into a Taylor series as

$$\varphi(\omega) = D_0 + D_1.(\omega - \omega_0) + D_2.(\omega - \omega_0)^2 + D_3.(\omega - \omega_0)^3 + \cdots. \tag{2}$$

Here, D_2 is the Group Delay Dispersion (GDD), and D_3 is the Third Order Dispersion (TOD). For a Fourier-limited laser pulse, the GDD and higher-order terms are zero, while a non-zero GDD lengthens the pulse and introduces a linear frequency chirp. A non-zero TOD introduces an asymmetry in the pulse shape and give rise to side pulses. This allows one to manipulate the CHG pulse shape by tuning the laser and chicane properties.

To study this effect and to compare the simulations with the observations made at DELTA short-pulse facility, the spectra of CHG radiation were simulated for laser pulses with different spectral laser phase and varying strengths R_{56} of the magnetic chicane. The influence of two laser pulse parameters, GDD and TOD, on the CHG spectra was primarily investigated. To predict their values from the measured CHG spectra, a Convolutional Neural Network (CNN) was designed and subsequently trained with a data set of over 40000 numerically simulated spectra for various combinations of GDD and TOD values [19]. With the trained surrogate model, GDD and TOD values of the seed laser pulse were predicted from the observed CHG spectra for different seed laser phases. Figure 7 compares two examples of observed CHG radiation intensities as a function of the emitted wavelength and the chicane strength (spectral map) with those simulated using the GDD and TOD values predicted by the CNN.

SUMMARY AND OUTLOOK

Collectively, all studies highlight the successful integration of machine ML techniques into accelerator physics applications, enabling improved control, efficiency, and precision across a variety of time-consuming and complex processes.

In some cases, the results can be further improved by additional parameter optimizations of the ML algorithms and by systematic extension of the training data. Here, incorporating 'online' training during machine operation ("training on the fly") and reinforcement learning techniques can be beneficial additions.

Furthermore, to enhance sampling of the prediction models, the future investigations of alternative optimization strategies such as swarm intelligence (e.g., Ant Colony Optimization) or other evolutionary-based algorithms is intended.

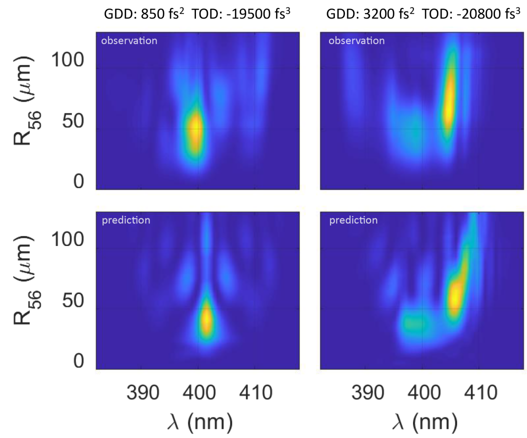

Figure 7: Observed CHG spectral maps (top row) and simulated spectral maps from the GDD and TOD values predicted by CNN (bottom row). The predicted GDD and TOD values are specified above each column.

One issue with the ML-based approach for CHG spectra analysis is that the simulated spectral maps are generated from idealized simulations which do not consider several factors such as the higher-order spectral phase beyond TOD, reflectivity and transmittance of the optical components used, noise in the observation etc. A better representation of these effects in the training samples could help the CNN achieve closer matches in the CHG spectral maps observed in practice.

Finally, it is planned to implement dedicated software containers for the more universal steps in the ML workflow to improve software maintenance and reusability.

ACKNOWLEDGEMENT

We would like to thank all colleagues of the DELTA team for many helpful suggestions as well as for providing sufficient data mining time during accelerator shifts. Special thanks to Andrè Althaus for his support with all control system issues.

REFERENCES

[1] M. Tolan, T. Weis, C. Westphal, and K. Wille, "DELTA: Synchrotron light in nordrhein-westfalen", *Synchrotron Radiat. News*, vol. 16, no. 2, pp. 9–11, 2003. doi:10.1080/08940880308603005

[2] S. Khan *et al.*, "Coherent Harmonic Generation at DELTA: A New Facility for Ultrashort Pulses in the VUV and THz Regime", in *Synchrotron Radiation News*, vol. 24, no. 5, pp. 18–23, 2011. doi:10.1080/08940886.2011.618092

[3] S. Khan *et al.*, "Generation of Ultrashort and Coherent Synchrotron Radiation Pulses at DELTA", *Synchrotron Radiation News*, vol. 26, no. 3, pp. 25–29, 2013. doi:10.1080/08940886.2013.791213

[4] M. Grewe, "SVD-basierte Orbitkorrektur am Speicherring Delta", dissertation, TU Dortmund, Germany, 2005.

ISBN: 978-3-95450-238-7 ISSN: 2226-0358 doi:10.18429/JACoW-ICALEPCS2023-TUPDP020

[5] S. Kötter, "Orbit Correction and Response Analysis at DELTA", dissertation, TU Dortmund, Germany, 2022.

[6] R. Fletcher and C. M. Reeves, "Function minimization by conjugate gradients", *Comput. J.*, vol. 7, pp. 149–154, 1964. doi:10.1093/comjnl/7.2.149

[7] M. F. Møller, "A scaled conjugate gradient algorithm for fast supervised learning", *Neural Networks*, vol. 6, no. 4, pp. 525–533, 1993. doi:10.1016/S0893-6080(05)80056-5

[8] D. Schirmer, "Orbit Correction With Machine Learning Techniques at the Synchrotron Light Source DELTA", in *Proc. ICALEPCS'19*, New York, NY, USA, Oct. 2019, pp. 1432. doi:10.18429/JACoW-ICALEPCS2019-WEPHA138

[9] D. Schirmer, A. Althaus, S. Hüser, S. Khan, T. Schüngel, "Machine learning projects at the 1.5–GeV synchroton light source DELTA", in *Proc. ICALEPCS'21*, Shanghai, China, 2021, pp. 631–635. doi:10.18429/JACoW-ICALEPCS2021-WEPV007

[10] D. Schirmer, "A machine learning approach to electron orbit control at the 1.5 GeV synchrotron light source DELTA", in *J. Phys.: Conf. Ser.*, vol. 2420, 2023, p. 012069. doi:10.1088/1742-6596/2420/1/012069

[11] P. Hartmann, J. Fuersch, R. Wagner, T. Weis, and K. Wille, "Kicker Based Tune Measurement for DELTA", in *Proc. DIPAC'07*, Venice, Italy, May 2007, paper WEPB21, pp. 277–279.

[12] D. Schirmer, A. Althaus, S. Hüser, S. Khan, and T. Schüngel, "New machine learning projects at DELTA", in *17th DELTA Annual Report 2021*, Dortmund, Germany, November 2021, pp. 3–4. https://www.delta.tu-dortmund.de/cms/Medienpool/User_Reports/DELTA_User_Report_2021.pdf

[13] D. Schirmer, "Machine learning applied to automated tunes control at the 1.5 GeV synchrotron light source DELTA", in *Proc. IPAC 2021*, Campinas, Brazil, 2021, pp. 3379–3382. doi:10.18429/JACoW-IPAC2021-WEPAB303

[14] T. Schüngel, "Development of a Container-Based Work Environment for an automated Optimization of the Sextupole Settings and Injection Efficiency using Machine-Learning at the Storage Ring DELTA", Master's Thesis, TU Dortmund, August 2022.

[15] D. Schirmer, A. Althaus, and T. Schüngel, "Machine learning methods for chromaticity control at the 1.5 GeV synchrotron light source DELTA", in *Proc. IPAC 2022*, Bangkok, Thailand, 2022, pp. 1141–1144. doi:10.18429/JACoW-IPAC2022-TUPOPT059

[16] S. Hüser, "Implementierung neuartiger Optimierungsalgorithmen an der Speicherringsanlage DELTA", Diploma Thesis, TU Dortmund, May 2022.

[17] D. Schirmer, A. Althaus, S. Hüser, S. Khan, and T. Schüngel, "Machine learning-based optimization of storage ring injection efficiency", in *Proc. of IPAC 2023*, Venice, Italy, 2023, pp. 2853–2856. doi:10.18429/JACoW-IPAC2023-WEPA106

[18] R. Coisson and F. De Martini, "Free-electron coherent relativistic scatterer for UV-generation", in *Phys. Quantum Electron.*, vol. 9, p. 939, 1982.

[19] A. Radha Krishnan, B. Büsing, A. Held, H. Kaiser, S. Khan, C. Mai, Z. Usfoor, and V. Vijayan, "Investigation of Spectro-Temporal Properties of CHG Radiation at DELTA", in *Proc. IPAC 2022*, Bangkok, Thailand, 2022, pp. 1423–1426. doi:10.18429/JACoW-IPAC2022-TUPOMS012